Extensional Strain Hardening Induced by π-π Interactions in Barely Entangled Polymer Chains: The Curious Case of Poly(4-vinylbiphenyl)

Carlos R. López-Barrón[1,*] and Huaxing Zhou[2]
[1]ExxonMobil Chemical Company, Baytown, Texas 77520, USA
[2]ExxonMobil Research and Engineering Company, Annandale, New Jersey 08801, USA

(Received 28 July 2017; revised manuscript received 12 October 2017; published 11 December 2017)

Aromatic π-π interactions between phenyl groups of adjacent chains in poly(4-vinylbiphenyl) (PVBP) have profound effects on the dynamics of this polymer. We report two unexpected nonlinear viscoelastic responses of PVBP when subjected to uniaxial flow. One is the unprecedented observation of extensional strain hardening (SH) in a barely entangled polymer melt. An even more intriguing finding is that SH of lightly (or even barely) entangled melts occurs at strain rates one order of magnitude below the coil-stretch transition predicted by Rouse theory ($\dot{\varepsilon}_H = 0.5/\tau_R$).We postulate that this behavior is due to a molecular rearrangement mechanism (supported by x-ray diffraction measurements) that involves flow-induced π-π stacking of the phenyl groups, which results in an enhancement of the friction coefficient between polymer chains.

DOI: 10.1103/PhysRevLett.119.247801

One of the most interesting nonlinear viscoelastic responses in entangled polymers is the so-called extensional "strain hardening" (SH) observed during strong elongational flows. SH manifests as the upward deviation of the transient extensional viscosity $\eta_E^+(t)$ measured at a finite rate from the zero-rate viscosity $3\eta_0^+(t)$ [where $\eta_0^+(t)$ is the zero-rate shear viscosity]. The strength of SH is a key parameter for the design of commercial polymers that undergo operations involving extensional flows (e.g., film blowing and foaming) [1]. However, despite the numerous studies focused on strong elongational flows [1–12], a universally accepted molecular mechanism for the SH phenomenon is still lacking. The most widely accepted hypothesis is that SH originates from stretching of the polymer chains occurring when the elongation rate $\dot{\varepsilon}_H$ exceeds the inverse of the stretch relaxation time [4]. The latter is given by the Rouse time τ_R for monodisperse polymers [13]. It has also been proposed that SH is due to "condensation" of entanglement strands to a reduced cross-sectional area during uniaxial extension [9]. Recently, another mechanism involving nematic interactions was proposed to explain the enhanced SH in blends of highly entangled polystyrene (PS) chains with unentangled (oligomeric) PS chains, when compared with neat PS melt with similar number of entanglements [8,10]. This is a plausible mechanism; however, the origin of such nematic interactions (consisting of short-range orientational coupling acting between oriented chains and surrounding free molecules [14]) has not been elucidated yet. An interesting question is whether such interactions depend on the identity of the monomeric units in the chain.

Another question that has not been addressed yet is whether unentangled polymer melts are able to undergo SH. Rouse theory predicts that as soon as the Rouse Weissenberg number $\mathrm{Wi}_R = \dot{\varepsilon}_H \tau_R > 0.5$ (i.e., above the coil-stretch transition), the chains undergo stretching, and could produce SH [7]. Therefore, based on this argument, entanglement of the chains in the melt is not a requirement for SH. However, to our knowledge, there is no previous evidence of any unentangled, or lightly entangled, polymer melt showing SH when subjected to elongational flow. Herein, we report the unusual nonlinear viscoelastic response, that includes strong SH, of entangled and barely entangled poly(4-vinyl biphenyl) (PBVP) samples subjected to uniaxial extensional flow. The synthesis, linear viscoelasticity and molecular structure of PVBP were recently reported [15]. The molecular characteristics of the samples studied here are shown in Table I. Samples PVBP71, PVBP171 PVBP507, and PVBP857 were synthesized by living anionic polymerization, whereas samples PVBP27 and PVBP120 were prepared by free radical polymerization. The number of entanglements per molecule is computed as $Z = M_n/M_e$, where M_e is the molecular weight between entanglements. For PVBP, $M_e = 58.3$ kg/mol, which is calculated from the measured rubbery plateau modulus ($G_N^0 = 0.065$ MPa) using the relation $M_e = \rho RT/G_N^0$ [15].

The longest Rouse relaxation time τ_R is the most relevant characteristic time for this study, as it determines the relation between chain stretching and stress response during uniaxial flow [4,13]. This parameter was estimated using the method developed by Osaki *et al.* [16], using Rouse theory. This method dictates that $\tau_R = (aM/1.111\rho RT)^2$, where the parameter a is obtained from the power law behavior followed by the storage modulus in the high frequency regime, just beyond the rubbery plateau modulus: $G'(\omega) = a\omega^{1/2}$. Power law fits to the $G'(\omega)$ data are shown in the Supplemental Material [17] and a comprehensive analysis of the linear viscoelastic behavior of these samples is reported elsewhere [15]. Values of τ_R measured at 170 °C and 190 °C

TABLE I. Molecular characteristics and Rouse relaxation time of PVBP samples.

				τ_R, s	
Sample ID	M_n, kg/mol	M_w/M_n	Z	170 °C	190 °C
PVBP71	71.2	1.08	1.22	104.7	1.43
PVBP171	171	1.12	2.93	1109	10.8
PVBP507	507	1.71	8.70	⋯	88.4
PVBP857	857	1.67	14.7	⋯	306
PVBP27	27.2	2.05	0.47	3.91	0.084
PVBP120	120	2.10	2.05	⋯	6.33

are tabulated in Table I. The inset in Fig. 1(b) shows that τ_R closely follows the power law relation with MW (or Z) predicted by Rouse theory: $\tau \sim N^2$. Note that the Rouse theory applies to melts of short unentangled chains, for which the storage and loss moduli are equal to each other and scale with the square root of frequency $[G'(\omega) \simeq G''(\omega) \sim \omega^{1/2}]$ for $1/\tau_R < \omega < 1/\tau_0$, where τ_0 is the monomer relaxation time [19]. Samples PVBP71, PVBP27, and PVBP120 show this behavior, as indicated in Fig. S1 of the Supplemental Material [17].

The nonlinear viscoelastic response to uniaxial deformation for the PVBP samples in the melt (at 170 °C and 190 °C) were obtained using a Sentmanat extensional rheometer (SER, Xpansion Instruments) mounted on a stress-controlled rheomether DHR-3 (TA Instruments). Note that none of our measurements reach the steady-flow state, due to early rupture of the specimens. Figure 1(a) shows $\eta_E^+(t)$ for the four PVBP samples with lower polydispersity (PDI) measured at 190 °C (measurements at 170 °C and for the rest of the polymers are given in the Supplemental Material [17]). The dashed lines represent the linear viscoelastic (LVE) predictions in the zero strain limit $[3\eta_0^+(t)]$, which are computed from the small amplitude oscillatory shear data, as described in the Supplemental Material [17]. The extensional rheology was measured at four Hencky strain rates ($\dot{\varepsilon}_H$). The data for all the samples collapse into a single line at $t < 0.1$ s, which is expected as this regime corresponds to the glass transition regime, which is, as reported recently [15], identical for all the samples, regardless their MW. For all the samples, the measured extensional viscosity are in good agreement with the LVE predictions at low strains ($\varepsilon_H = \dot{\varepsilon}_H \cdot t < 1$). However, they all show an upward deviation (SH) at $\varepsilon_H > 1$. As discussed above, this is not unexpected for the entangled samples, when they are stretched at a $\mathrm{Wi}_R > 0.5$, i.e., above the coil-stretch transition. However, this is not the case for all of the experiments reported here.

In order to quantify the level of deviation from the LVE predictions, we define the strain hardening ratio (SHR) as the ratio between the extensional viscosity and the LVE prediction, both measured at $\varepsilon_H = 3$. Figure 1(b) displays SHR as a function of Wi_R for all the experiments run on the six samples listed in Table I, including four strain rates and two temperatures (170 °C and 190 °C). In the range of $\mathrm{Wi}_R < \sim 20$ the SHR data show a monotonic increase with deformation rate, described by a power law: $\mathrm{SHR} \sim \mathrm{Wi}_R^b$ (with exponent $b \sim 1/3$). At $\mathrm{Wi}_R > 20$, SHR becomes independent of the deformation rate. In this regime SHR is also independent of MW, which is evident in Fig. 1(a) where the data for all the samples measured at $\dot{\varepsilon}_H = 10\ \mathrm{s}^{-1}$ overlap in a single curve. Figure 1(b) includes data for an entangled polystyrene (PS) sample, for which $Z = 8.3$ (using $M_e = 13.3$ kg/mol [20]), measured at 120 °C, at which $\tau_R = 132$ s. The extensional viscosity data for the PS sample are given in the Supplemental Material [17]. The

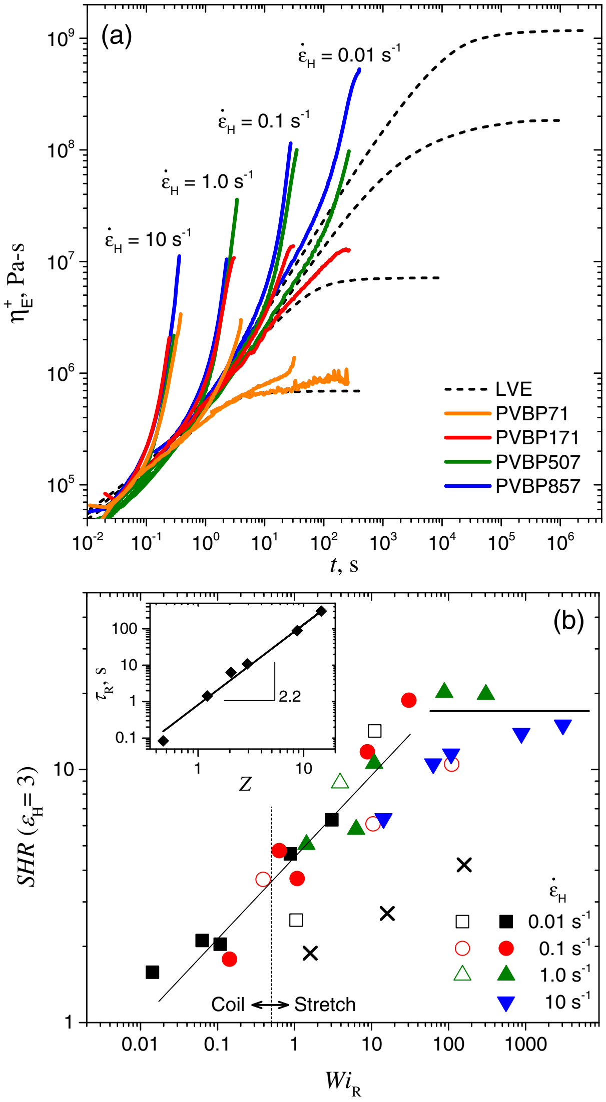

FIG. 1. (a) Transient extensional viscosity during startup of extensional flow for the low PDI samples measured at 190 °C and at the indicated strain rates. (b) SHR versus Wi_R for all the samples for all the PVBP samples measured at 170 °C (open symbols) and 190° (closed symbols), and for a PS sample (with $Z = 8.3$) measured at 120 °C (crosses). Inset: τ_R values measured at 190 °C versus Z.

much (3 to 4 times) lower SHR values measured in PS, compared to those measured in PVBP, evinces the strong effect of the aromatic π-π interactions in the elongational behavior for PVBP, as discussed below.

The most interesting feature in Fig. 1(b) is the fact that SH is observed at Wi_R values as low as 0.014, which is more than an order of magnitude lower than the value corresponding to the coil-stretch transition ($\mathrm{Wi}_R = 0.5$), predicted by Rouse theory. [7] This seems to contradict the current believe that SH is a direct consequence of chain stretching, which would only occurs at deformation where $\mathrm{Wi}_R > 0.5$. Hence, the questions that arises from these observations is whether, for the particular case of PVBP, the coil-stretch transition occurs at very low Wi_R values? Or if uniaxial extension activates an additional friction mechanism that produces SH that is not associated with chain stretching? As discussed below, x-ray diffraction measurements allows us to elucidate these questions.

An even more intriguing response in the PVBP samples is illustrated in Fig. 2, which shows plots of transient extensional viscosity for two samples that are barely entangled. Note that the LVE response of these two samples is that of unentangled melts described by the Rouse model (see Fig. S1), although their molecular weight distributions [displayed in Fig. 2(c)] show a small tail with $Z \sim 2-4$. Remarkably, both samples show SH, not only at $\mathrm{Wi}_R > 0.5$, but also at strain rates way below the coil-stretch transition, which is in direct contradiction with Rouse theory. Refined models based on Doi-Edward tube model, [13] predict that in the fast deformation regime chain relaxation is controlled by the Rouse-like friction, and therefore, entanglements are, in fact, irrelevant (although they may still act as potential topological obstacles) [21,22]. Therefore, tube theory does not fundamentally forbid chain stretching and the concomitant SH in unentangled polymers. However, to our knowledge, this is the first report of SH measured on a barely entangled polymer melt.

To elucidate the mechanism of SH in PVBP, we performed wide-angle x-ray scattering (WAXS) on the sample PVBP120 using a SAXSLAB instrument (Ganesha 300XL) equipped with a 2D detector (Dectris Pilatus 300K). Distances were calibrated using silver behenate, using the program SAXSGUI (JJ X-Ray Systems ApS). Two samples were prepared for the WAXS measurements. One was annealed for 30 min in an oven at 200°C with nitrogen environment to avoid thermal degradation. A second sample was prepared by stretching it in the SER (mounted in the DHR rheometer) at a rate of $\dot{\varepsilon}_H = 0.01\ \mathrm{s}^{-1}$, and quenching it by submerging the whole sample (and the SER drums) in liquid nitrogen *during* the last two seconds of deformation before reaching a strain of $\varepsilon_H = 2.4$. Note that this quenching procedure completely eliminates the possibility of any molecular relaxation during quenching. WAXS data for these two samples are shown in Fig. 3(a). Two main isotropic broad diffraction peaks are observed in the annealed sample at the q positions (where q is the scattering wave vector), labeled as q_1^* and q_2^*. The x-ray diffraction profile of PVBP was reported in a recent publication [15], where it was determined that the peak at q_1^* arises from interchain (backbone-to-backbone) correlations and the peak at q_2^* from interaction between adjacent phenyl groups (aromatic π-π interactions) from neighbor chains. This is schematically illustrated in Fig. 4(a), where the characteristic distances are computed as $d_i = 2\pi/q_i^*$ ($i = 1\ldots4$). Note that the interphenyl peak can be deconvoluted into two peaks, at q_2^* and q_3^*, which correspond to T-shaped (T) and parallel-displacement (PD) π-π configuration, respectively. An additional peak at q_4^* results from the correlation between adjacent phenyl groups attached to the backbone [15].

The 2D WAXS profile of the stretched sample shows anisotropy in both peaks, which is better visualized in the plot of scattering intensity as a function of azimuthal angle, ϕ [Fig. 3(b)]. For the inter-chain peak, the scattering intensity is concentrated in equatorial regions, perpendicular to the SD. This indicates that the chain backbones stretch in the SD. Such stretching is not expected, as the strain rate applied to this sample correspond to $\mathrm{Wi}_R = 0.06$ (an order of magnitude below the coil-stretch transition). On the other hand, the intensity of the interphenyl peak is concentrated

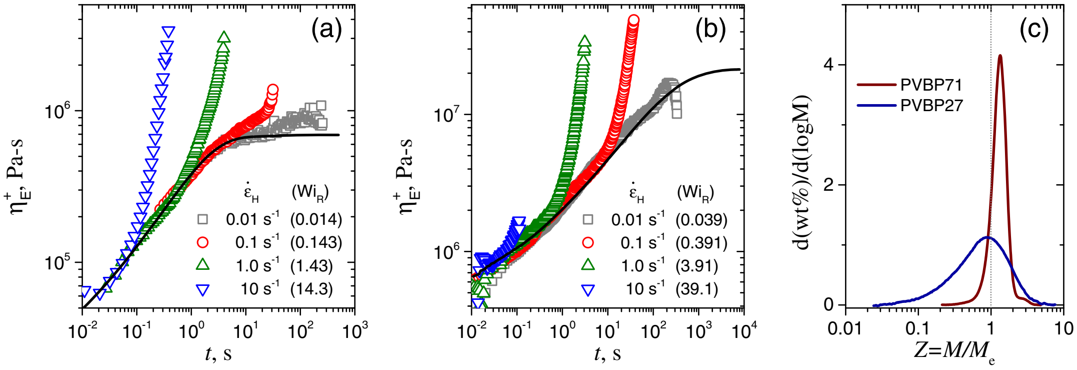

FIG. 2. Transient extensional viscosity for (a) PVBP71 measured at 190 °C and for (b) PVBP27 measured at 170 °C. Solid lines are LVE predictions. The MWD of these two samples are shown in (c).

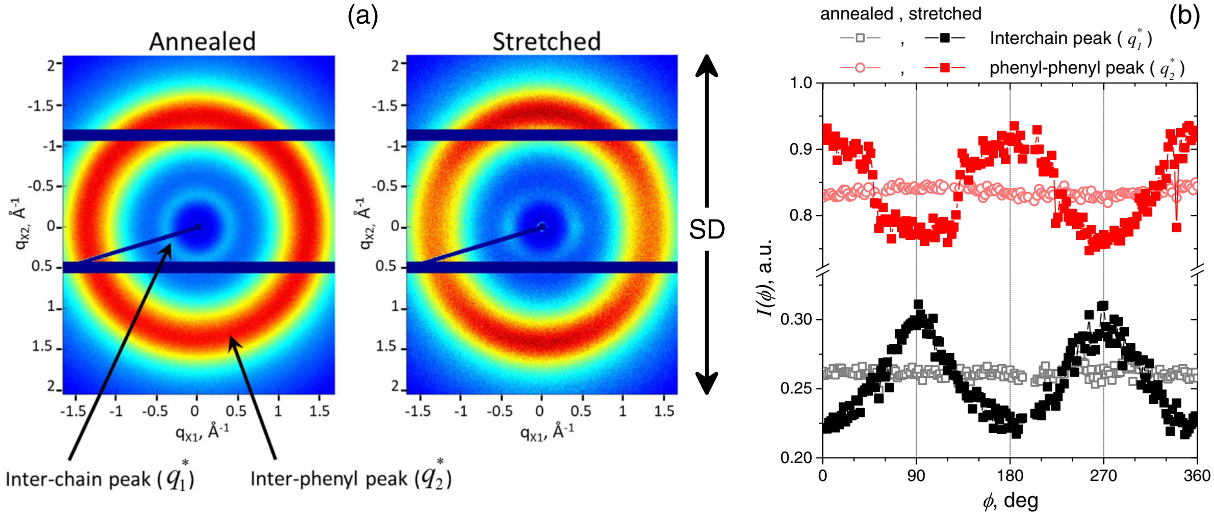

FIG. 3. (a) 2D WAXS patterns of the annealed and stretched PVBP120 sample. (b) Annular averaged intensity versus azimuthal angle for the annealed and stretched sample. The averaging is performed using the data corresponding to the ring sectors spanning the q ranges from 0.32 to 0.64 Å^{-1} (for the interchain peak) and from 1.25 to 1.7 Å^{-1} (for the phenyl-phenyl peaks).

along the SD, indicating stronger interaction between phenyl groups along SD and weaker interactions along the transverse direction (TD). This can be rationalized as follows. By pulling the backbone chains in the SD, the pending biphenyl groups are forced to adopt a perpendicular configuration where the axes of the planar phenyl rings, along which its π system resonates, point toward the SD (as illustrated in Figure 4(a)). In this configuration the external phenyl rings are prone to pack into stronger π-π stacking units, which would result in increased friction between PVBP chains. We postulate that this strain-induced π-π stacking, and the concomitant friction coefficient increase, is the main mechanism for the unusual SH observed at low strain rates.

To better understand the structural rearrangement in PVBP upon uniaxial deformation, 1D plots of the intensity versus q are displayed in Fig. 4(b). The data are measured on 40° angular sectors aligned along both SD and TD [see inset in Fig. 4(b)] for the stretched sample and compared to the scattering profile of the annealed sample. Besides the obvious differences in intensity, discussed above, slight changes in peak positions are also evident. The characteristic distances, computed from the peak positions, are listed in Table II. These data reveal several structural rearrangements resulting from uniaxial extension of PVBP:

(i) The distance between backbones (d_1) is notably reduced in the direction perpendicular to the flow (~9% reduction). This observation is in qualitative agreement with the SH mechanism proposed by Liu *et al.* [9], based on reduction of the cross-sectional area (condensation) during uniaxial extension.

(ii) The distance between phenyl groups (d_2) is reduced by ~5% in the flow direction. This is a direct consequence of (i), as the approach of adjacent backbones forces the phenyl groups to be closer together. Note that in the

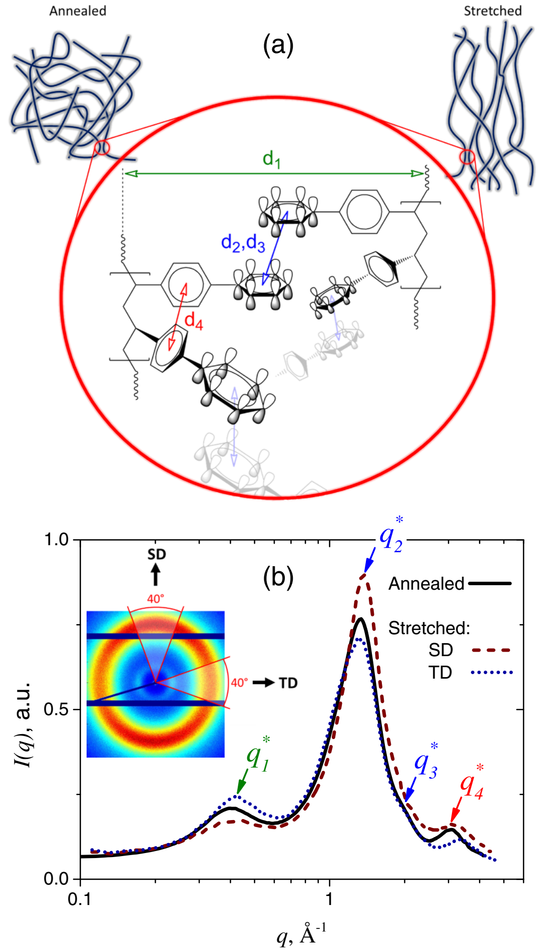

FIG. 4. (a) Cartoon of PVBP chains annealed and stretched showing schematically a detail of the characteristic distances measured by WAXS. (b) 1D WAXS profile of the annealed and stretched PVBP120 sample. The inset show the angular sectors used for the SD and TD averaged profiles.

TABLE II. Characteristic distances for the annealed and stretched PVBP120 sample computed from the diffraction peak positions, as $d_i = 2\pi/q_i^*$.

Sample	d_1	d_2	d_3	d_4
Annealed	15.7	4.73	1.94	2.12
Stretched (SD)	15.4	4.52	⋯	2.03
Stretched (TD)	14.4	4.75	⋯	1.93

annealed sample, phenyl rings from adjacent chains overlap (in average) a distance $d_{\mathrm{overlap}} \sim 2$ Å (computed as $d_{\mathrm{overlap}} = 2L_{\mathrm{biphenyl}} - d_1$, where $L_{\mathrm{biphenyl}} = 8.7$ Å is the total length of a biphenyl group), which is roughly half the length of a phenyl ring [15]. For the stretched sample $d_{\mathrm{overlap}} \sim 3$ Å. This significant overlap increase contributes to the increment in chain friction upon stretching.

(iii) The distance between phenyl groups adjacent to the backbone (d_4) decreases in ~9%, as those phenyl groups are forced to approach to each other when the backbone is stretched in the direction of flow. Despite being intriguing, the decrease in d_4 has no consequences on the dynamics of PVBP melt, as these phenyl groups do not contribute to the friction between adjacent chains.

In summary, this Letter presents two unexpected features of the nonlinear viscoelastic response of PVBP. One is the first observation of SH in a barely entangled polymer melt. More intriguingly is the observation of SH at strain rates more than 1 order of magnitude below the theoretical coil-stretch transition, even for the slightly entangled melts. Although these results seem to contradict Rouse theory, we propose a molecular mechanism that is particular to the microstructure of PVBP. This involves strain-induced π-π stacking of the phenyl groups nonadjacent to the chain backbones. WAXS measurements suggest that extensional flow produces condensation of the chains, as proposed by Liu *et al.*, [9] which in turn increases the phenyl-phenyl overlap distance and ultimately increases the friction between adjacent chains. Note that this mechanism is not likely to operate in polystyrene melts as the phenyl groups in that polymer do not overlap, as recently reported [15]. However, one could argue that, due to the π-π interactions between phenyl rings of adjacent chains, the proposed nematic interactions [10] would be stronger in PS than in polymers that have no phenyl rings (such as polypropylene) but weaker than in PBVP due to the overlapping. Comparison between the nonlinear responses of those three classes of polymer is warranted to elucidate the origin of the nematic interactions proposed by Huang *et al.* [10]

The authors wish to thank Truyen Pham and Trent Mouton for assistance with rheological measurements, and to Joseph Throckmorton for assistance with x-ray measurements.

---

[*]Corresponding author.
carlos.r.lopez-barron@exxonmobil.com

[1] P. Spitael and C. W. Macosko, Polym. Eng. Sci. **44**, 2090 (2004).

[2] J. K. Nielsen, H. K. Rasmussen, O. Hassager, and G. H. McKinley, J. Rheol. **50**, 453 (2006).

[3] Y. Wang, S. Q. Wang, P. Boukany, and X. Wang, Phys. Rev. Lett. **99**, 237801 (2007).

[4] D. Auhl, P. Chambon, T. C. B. McLeish, and D. J. Read, Phys. Rev. Lett. **103**, 136001 (2009).

[5] Y. Wang, S. Cheng, and S. Wang, J. Rheol. **55**, 1247 (2011).

[6] T. Yaoita, T. Isaki, Y. Masubuchi, H. Watanabe, G. Ianniruberto, and G. Marrucci, Macromolecules **45**, 2773 (2012).

[7] O. Hassager, K. Mortensen, A. Bach, K. Almdal, H. K. Rasmussen, and W. Pyckhout-Hintzen, Rheol. Acta **51**, 385 (2012).

[8] Q. Huang, O. Mednova, H. K. Rasmussen, N. J. Alvarez, A. L. Skov, K. Almdal, and O. Hassager, Macromolecules **46**, 5026 (2013).

[9] G. Liu, H. Sun, S. Rangou, K. Ntetsikas, A. Avgeropoulos, and S. Wang, J. Rheol. **57**, 89 (2013).

[10] Q. Huang, N. J. Alvarez, Y. Matsumiya, H. K. Rasmussen, H. Watanabe, and O. Hassager, ACS Macro Lett. **2**, 741 (2013).

[11] G. Ianniruberto, Macromolecules **48**, 6306 (2015).

[12] C. R. López-Barrón, Y. Zeng, and J. J. Richards, J. Rheol. **61**, 697 (2017).

[13] M. Doi and S. F. Edwards, *The Theory of Polymer Dynamics* (Clarendon Press, Oxford University Press, Oxford, Oxfordshire, New York, 1986), p. 73.

[14] J. A. Kornfield, G. G. Fuller, and D. S. Pearson, Macromolecules **22**, 1334 (1989).

[15] C. R. López-Barrón, H. Zhou, J. M. Younker, and J. A. Mann, Macromolecules **50**, 9048 (2017).

[16] K. Osaki, T. Inoue, T. Uematsu, and Y. Yamashita, J. Polym. Sci. B **39**, 1704 (2001).

[17] See Supplemental Material at http://link.aps.org/supplemental/10.1103/PhysRevLett.119.247801 for linear viscoelasticity analysis and complementary extensional viscosity plots, which contains Ref. [18].

[18] M. Baumgaertel and H. H. Winter, Rheol. Acta **28**, 511 (1989).

[19] M. Rubinstein and R. H. Colby, *Polymer physics* (Oxford University Press, Oxford, New York, 2003), Vol. xi, p. 440.

[20] L. J. Fetters, D. J. Lohse, D. Richter, T. A. Witten, and A. Zirkel, Macromolecules **27**, 4639 (1994).

[21] D. Pearson, E. Herbolzheimer, N. Grizzuti, and G. Marrucci, J. Polym. Sci. B **29**, 1589 (1991).

[22] G. Ianniruberto and G. Marrucci, J. Rheol. **45**, 1305 (2001).